

Published in final edited form as:

Science. 2009 February 13; 323(5916): 940–943. doi:10.1126/science.1166112.

A Neural Mechanism for Microsaccade Generation in the Primate Superior Colliculus†

Ziad M. Hafed^{1,*}, Laurent Goffart², and Richard J. Krauzlis¹

¹*Systems Neurobiology Laboratory, Salk Institute for Biological Studies, 10010 N. Torrey Pines Road, La Jolla, 92037, USA*

²*INCM, DyVA, UMR 6193, CNRS - Aix-Marseille Universités, Marseille, France*

Abstract

During fixation, the eyes are not still, but often exhibit microsaccadic movements. The function of microsaccades is controversial, largely because the neural mechanisms responsible for their generation are unknown. Here we show that the superior colliculus (SC), a retinotopically organized structure involved in voluntary-saccade target selection, plays a causal role in microsaccade generation. Neurons in the foveal portion of the SC increase their activity before and during microsaccades with sizes of only a few minutes of arc, and exhibit selectivity for the direction and amplitude of these movements. Reversible inactivation of these neurons significantly reduces microsaccade rate without otherwise compromising fixation. These results, coupled with computational modeling of SC activity, demonstrate that microsaccades are controlled by the SC, and explain the link between microsaccades and visual attention.

Microsaccades are the very small (typically <12 min arc), involuntary, fast eye movements that occur during fixation (1-3). The behavioral properties and functional significance of microsaccades have been extensively studied - and sometimes vigorously debated - for many years (1-14). However, the neural mechanisms responsible for their generation are unexplored. We now show that the superior colliculus (SC), a retinotopically organized structure known to be important for selecting and initiating voluntary eye movements (15-17), is also part of the neural mechanism that controls microsaccades.

We analyzed SC activity associated with 15,205 microsaccades that occurred while monkeys fixated a small stationary spot (18). Each fixation trial lasted for 3,500 ms resulting in many microsaccades with a variety of directions and amplitudes (Fig. 1A, Supp. Fig. S1). These movements had dynamics like those of larger saccades (3) (Supp. Fig. S1A), consistent with evidence that pre-motor neurons (downstream from the SC) are active during movements as small as 12-15 min arc (19).

We targeted neurons in the rostral pole of the SC, which represents foveal goal locations (18, 20). Figure 1A shows the spiking activity of a neuron in the left SC during a single trial containing 9 microsaccades (highlighted in green). The neuron exhibited changes in activity that were correlated with microsaccades. For example, the microsaccades labeled 1 and 2 in Fig. 1A were predominantly downward and leftward, respectively, and both were associated with a reduction in the neuron's activity. In contrast, small, predominantly rightward

†This manuscript has been accepted for publication in **Science**. This version has not undergone final editing. Please refer to the complete version of record at <http://www.sciencemag.org/>. The manuscript may not be reproduced or used in any manner that does not fall within the fair use provisions of the Copyright Act without the prior, written permission of AAAS.

*To whom correspondence should be addressed. E-mail: zhafed@salk.edu.

microsaccades, such as the ones labeled 3 and 4, caused an increase in activity before microsaccade onset and a burst during the movement itself. Thus, the neuron preferred particular microsaccade directions and amplitudes. We characterized these preferences across all microsaccades by plotting the neuron's activity as a function of the two-dimensional microsaccade amplitude, and we found consistent increases in activity for predominantly rightward microsaccades (Fig. 1B, Neuron a). We also inspected the time-course of the neuron's microsaccade-related activity. For this analysis, we included only microsaccades along the neuron's preferred axis (shaded region in Fig. 1B), to highlight activity associated with the preferred and non-preferred directions, and sorted the movements by radial amplitude to facilitate visualization (Fig. 1C). The neuron's activity was remarkably similar to the stereotypical saccade-related activity observed in caudal "buildup" neurons (21) during large "macro" saccades (see Fig. S4, top, for samples), except that it happened for the smallest detectable eye movements.

Each neuron from the rostral SC exhibited individual preferences for a range of microsaccade directions and amplitudes. Figure 1D-G shows the activity of two additional sample neurons (Neurons b and c), again recorded from the left SC, that preferred movements to the lower right quadrant. Neuron b showed a peak in discharge for ~6 min arc amplitudes and reduced its activity for smaller and larger movements. Thus, Neuron b was tuned for saccade amplitudes smaller than those preferred by Neuron a, and also increased its activity for small leftward (i.e. ipsilateral) movements (Fig. 1D). Neuron c was tuned for amplitudes larger than those preferred by Neuron a, and increased its discharge for progressively larger microsaccades, up to ~44 min arc (Fig. 1F) (22).

Data from our population of neurons indicated that the SC contains a continuous representation of saccade amplitude and direction down to the smallest eye movements. We measured the activity of each neuron as a function of microsaccade amplitude along its preferred direction, and sorted the neurons based on their preferred microsaccade amplitudes (Fig. 2A). Neurons tiled the contralateral space of all measured microsaccade amplitudes, and included some neurons whose activity was highest for ipsilateral movements as well. The raw activity of one of these neurons preferring ipsilateral microsaccades (labeled Neuron d in Fig. 2A) is shown in Fig. S2. The presence of such activity indicates that microsaccades involve activity distributed across the two SCs, functionally bridging the two visual hemi-fields to represent central targets.

Consistent with a continuous spatial representation throughout the SC (21), neuronal activity during microsaccades sometimes extended to small, voluntary saccades. Figure 2B illustrates this for the three sample neurons of Fig. 1 by plotting their activity as a function of amplitude during microsaccades, as well as during larger visually-guided saccades. This figure uses a logarithmic x-axis scale to magnify the representation of small microsaccades for easier visualization. Neurons a and b in Fig. 1 were specifically tuned for movements with amplitudes classically associated with microsaccades, but Neuron c was active for amplitudes that also included some voluntary movements larger than microsaccades. Similar observations were made for the remainder of our population. Neurons active during both microsaccades and voluntary saccades generally preferred voluntary saccades less than ~5 deg in amplitude (Fig. S3). Neurons more caudal in the SC map (those preferring ~10 deg voluntary saccades in our data set) did not exhibit microsaccade-related activity (Fig. S4).

SC activity during microsaccades was also distinct from modulations caused by small deviations of eye position from the fixated goal (23) (Fig. S5), and it persisted in the absence of a visual stimulus (Fig. S6).

We next investigated if the SC is causally involved in microsaccade generation. Figure 3A shows the distribution of microsaccade occurrences during one second of steady-state fixation before and after reversibly inactivating a sample SC site. Inactivation caused a reduction in microsaccade rate ($p = 0.0003$; ranksum test), and this was consistent across sessions - except when the inactivated SC neurons represented eccentricities larger than ~ 5 -6 deg (Fig. 3B). This is consistent with our neuronal recordings showing a lack of microsaccade-related modulations for peripheral SC neurons (Fig. S4). Inactivation reduced the probability of both contralateral and ipsilateral microsaccades (Fig. 3C), again consistent with our neuronal data showing activity for both contralateral and ipsilateral movements. Thus, rostral SC activity is directly involved in microsaccade generation.

A computational model, in which “buildup” neurons in the rostral SC encode foveal goal locations (24,20), provides a plausible mechanism for microsaccade generation (Fig. 4A). During steady-state fixation, the selected goal is foveal and results in bilateral activity centered on neurons representing the central visual field. The instantaneous locus of this activity may be viewed as a stochastic process with zero mean (Fig. 4B). According to this model, microsaccades are triggered when the center of mass of SC activity deviates sufficiently from zero.

Our model explains the inactivation-induced reduction in microsaccades. We simulated the effects of inactivation by eliminating the activity of a subset of model neurons (Fig. 4C, arrow 1). In steady-state, inactivation reduces activity even on the intact side of the SC, without creating an imbalance across the right and left SC (24) (Fig. 4C). Thus, with the same stochastic processes influencing SC activity, the locus of the center of mass of this activity is less variable, reducing the probability of deviation beyond the threshold for triggering saccades (Fig. 4D). Because the activity remains balanced bilaterally (24) (Fig. 4C,D), inactivation reduces the frequency of both contralateral and ipsilateral microsaccades.

Our model can also explain why microsaccades are influenced by covert attention shifts (8, 9). Cognitive factors such as attention and prior expectations alter “buildup” neuron activity (25,26); these changes could bias SC activity sufficiently to cause asymmetries in microsaccade generation. We therefore simulated the momentary effects on SC activity of attending to a peripheral location (Fig. 4E). These effects caused the average locus of SC activity to shift slightly towards the peripheral site, resulting in a higher probability of supra-threshold deviations towards the “attended” location (Fig. 4F).

Our results provide a description of the neural mechanisms for generating saccades smaller than 12 min arc. Coupled with the report that pre-motor neurons in the brainstem reticular formation are active during saccades as small as 12-15 min arc (19), our results demonstrate that microsaccades share the same neural mechanisms as voluntary saccades. Our proposal that microsaccade occurrence depends on the variability of SC activity representing salient goal locations reconciles seemingly disparate observations about microsaccades. Because SC activity can be manipulated by task set as well as by shifts of attention (25,26), this interpretation can explain why microsaccades might be voluntarily suppressed in some conditions (6) but asymmetrically increased in others (8,9) (Fig. 4F). Our interpretation also suggests that microsaccades may be part of a visual feedback loop. If the variability in target-related activity increases because of perceptual fading (12), the resulting microsaccades would correct for this fading through their influence on visual cortical activity (27-30). This in turn reduces the variability of SC signals defining the fixated target location. This mechanism can explain the increases in microsaccade rate and variability during fixation with no visual stimuli (6,10), as well as the behavioral correlations between increases or decreases in microsaccade rates and intensifying or fading visual percepts (12).

Supplementary Material

Refer to Web version on PubMed Central for supplementary material.

Acknowledgements

Funding provided by NIH Grant EY12212 and Agence Nationale de la Recherche Grant RETINAE. We thank K. Nielsen and V. Ciaramitaro for helpful comments.

References and Notes

1. Barlow HB. *J. Physiol. (Lond.)* 1952;116:290–306. [PubMed: 14939180]
2. Steinman RM, Haddad GM, Skavenski AA, Wyman D. *Science* 1973;181:810–819. [PubMed: 4198903]
3. Zuber BL, Stark L, Cook G. *Science* 1965;150:1459–1460. [PubMed: 5855207]
4. Bridgeman B, Palca J. *Vision Res* 1980;20:813–817. [PubMed: 7456343]
5. Kingstone A, Fendrich R, Wessinger CM, Reuter-Lorenz PA. *Percept. Psychophys* 1995;57:796–801. [PubMed: 7651804]
6. Steinman RM, Cunitz RJ, Timberlake GT, Herman M. *Science* 1967;155:1577–1579. [PubMed: 6020487]
7. Winterson BJ, Collewijn H. *Vision Res* 1976;16:1387–1390. [PubMed: 1007017]
8. Hafed ZM, Clark JJ. *Vision Res* 2002;42:2533–2545. [PubMed: 12445847]
9. Engbert R, Kliegl R. *Vision Res* 2003;43:1035–1045. [PubMed: 12676246]
10. Cornsweet TN. *J. Opt. Soc. Am* 1956;46:987–993. [PubMed: 13367941]
11. Kowler E, Steinman RM. *Vision Res* 1980;20:273–276. [PubMed: 7385602]
12. Martinez-Conde S, Macknik SL, Troncoso XG, Dyar TA. *Neuron* 2006;49:297–305. [PubMed: 16423702]
13. Ratliff F, Riggs LA. *J. Exp. Psychol* 1950;40:687–701. [PubMed: 14803643]
14. Martinez-Conde S, Macknik SL, Hubel DH. *Nat. Rev. Neurosci* 2004;5:229–240. [PubMed: 14976522]
15. McPeck RM, Keller EL. *Nat. Neurosci* 2004;7:757–763. [PubMed: 15195099]
16. Carello CD, Krauzlis RJ. *Neuron* 2004;43:575–583. [PubMed: 15312655]
17. Krauzlis RJ. *J. Neurosci* 2003;23:4333–4344. [PubMed: 12764122]
18. Materials and Methods, including behavioral tasks, single-neuron recordings, and inactivations, are available as supporting material on *ScienceOnline*
19. Van Gisbergen JAM, Robinson DA, Gielen SA. *J. Neurophysiol* 1981;45:417–442. [PubMed: 7218009]
20. Hafed ZM, Krauzlis RJ. *J. Neurosci* 2008;28:9426–9439. [PubMed: 18799675]
21. Munoz DP, Wurtz RH. *J. Neurophysiol* 1995;73:2313–2333. [PubMed: 7666141]
22. Because microsaccades are not under full experimental control, they posed special challenges, described in more detail in the supporting material “Microsaccade detection and analysis” on *ScienceOnline*
23. Krauzlis RJ, Basso MA, Wurtz RH. *J. Neurophysiol* 2000;84:876–891. [PubMed: 10938314]
24. Hafed ZM, Goffart L, Krauzlis RJ. *J. Neurosci* 2008;28:8124–8137. [PubMed: 18685037]
25. Ignashchenkova A, Dicke PW, Haarmeier T, Thier P. *Nat. Neurosci* 2004;7:56–64. [PubMed: 14699418]
26. Basso MA, Wurtz RH. *J. Neurosci* 1998;18:7519–7534. [PubMed: 9736670]
27. Martinez-Conde S, Macknik SL, Hubel DH. *Nature Neurosci* 2000;3:251–258. [PubMed: 10700257]
28. Leopold DA, Logothetis NK. *Exp. Brain Res* 1998;123:341–345. [PubMed: 9860273]
29. Snodderly DM, Kagan I, Gur M. *Vis. Neurosci* 2001;18:259–277. [PubMed: 11417801]
30. Bair W, O’Keefe LP. *Vis. Neurosci* 1998;15:779–786. [PubMed: 9682878]

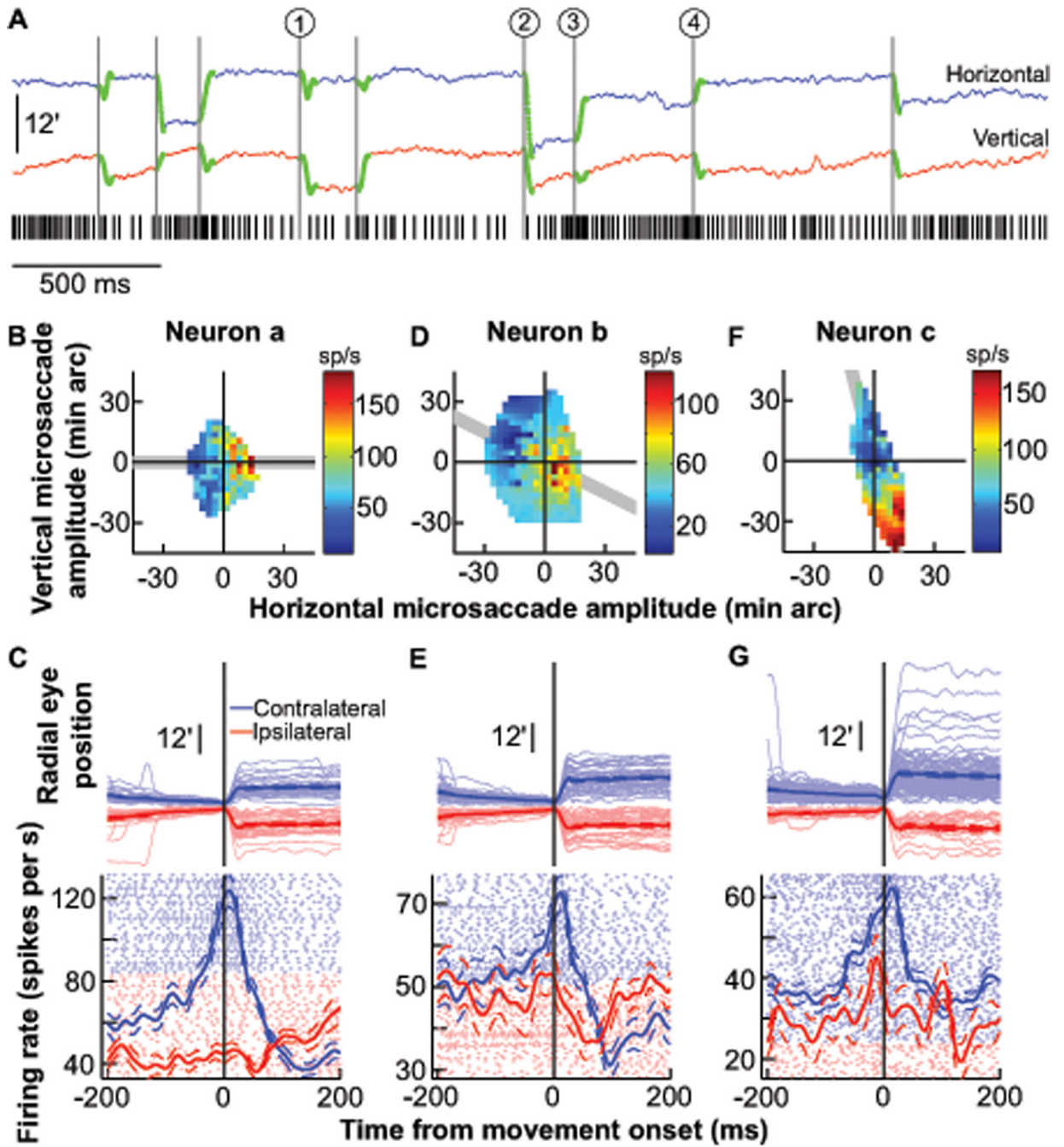


Fig. 1. Microsaccade-related activity in the SC. **A**, Sample trial from one neuron. Microsaccades are highlighted in green on the eye position traces (18); the black tick marks indicate the neuron's spike times. The circled numbers highlight sample microsaccades that were associated with either a reduction in the neuron's activity (1 and 2) or a gradual buildup until movement onset (3 and 4). Upward deflections in the eye position traces denote right or up. **B**, Peak discharge of the same neuron during all microsaccades plotted as a function of their horizontal and vertical amplitudes. The neuron preferred rightward movements. **C**, Radial eye positions and neuronal activity for all microsaccades in the shaded gray region of **B** for the same neuron. Data are aligned on microsaccade onset and sorted by radial amplitude for contralateral (light blue) and

ipsilateral (light red) movements. The vertical starting positions for successive microsaccade traces are also aligned, but slightly offset from each other (by 0.06 min arc each), to facilitate visualization. Blue and red show average eye position or firing rate (with s.e.m. envelopes). Light-colored dots show individual-movement spike rasters. **D, E**, Similar to **B, C** but for another neuron, recorded from the same SC side, which preferred smaller movements directed to the lower right quadrant. **F, G**, Similar to **B, C** but for a third neuron, from the same SC side, preferring larger movements (22).

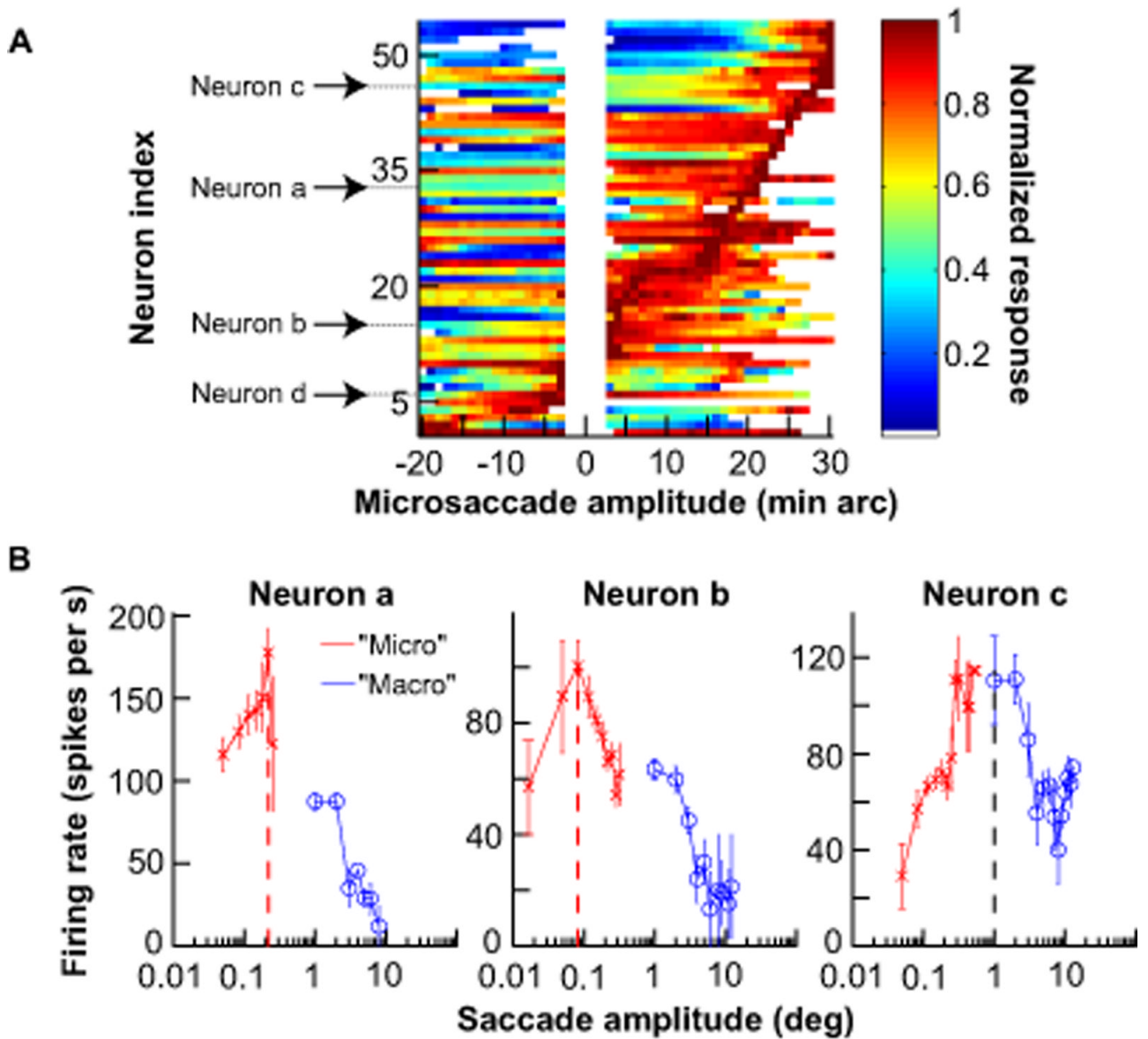


Fig. 2.

Continuum of SC activity down to the smallest detectable saccades. **A**, Peak discharge of each neuron during microsaccades plotted as a function of microsaccade amplitude along the neuron's preferred direction (positive is contralateral). Neurons are sorted based on the amplitude that caused peak activity. Labeled neurons are the sample neurons of Fig. 1 and Fig. S2 (Neuron d). White space in middle indicates unanalyzed bins (18). Each shown bin contains at least 5 microsaccades. **B**, Comparison of neuronal activity during contralateral microsaccades along the neurons' preferred directions with activity during larger contralateral voluntary saccades. Some neurons were specifically tuned for microsaccades, and paused or significantly reduced their activity for larger "macro" saccades (Neurons a and b). Other neurons continued to increase their discharge for slightly larger saccades (Neuron c, Supp. Fig. S3). Error bars denote s.e.m.

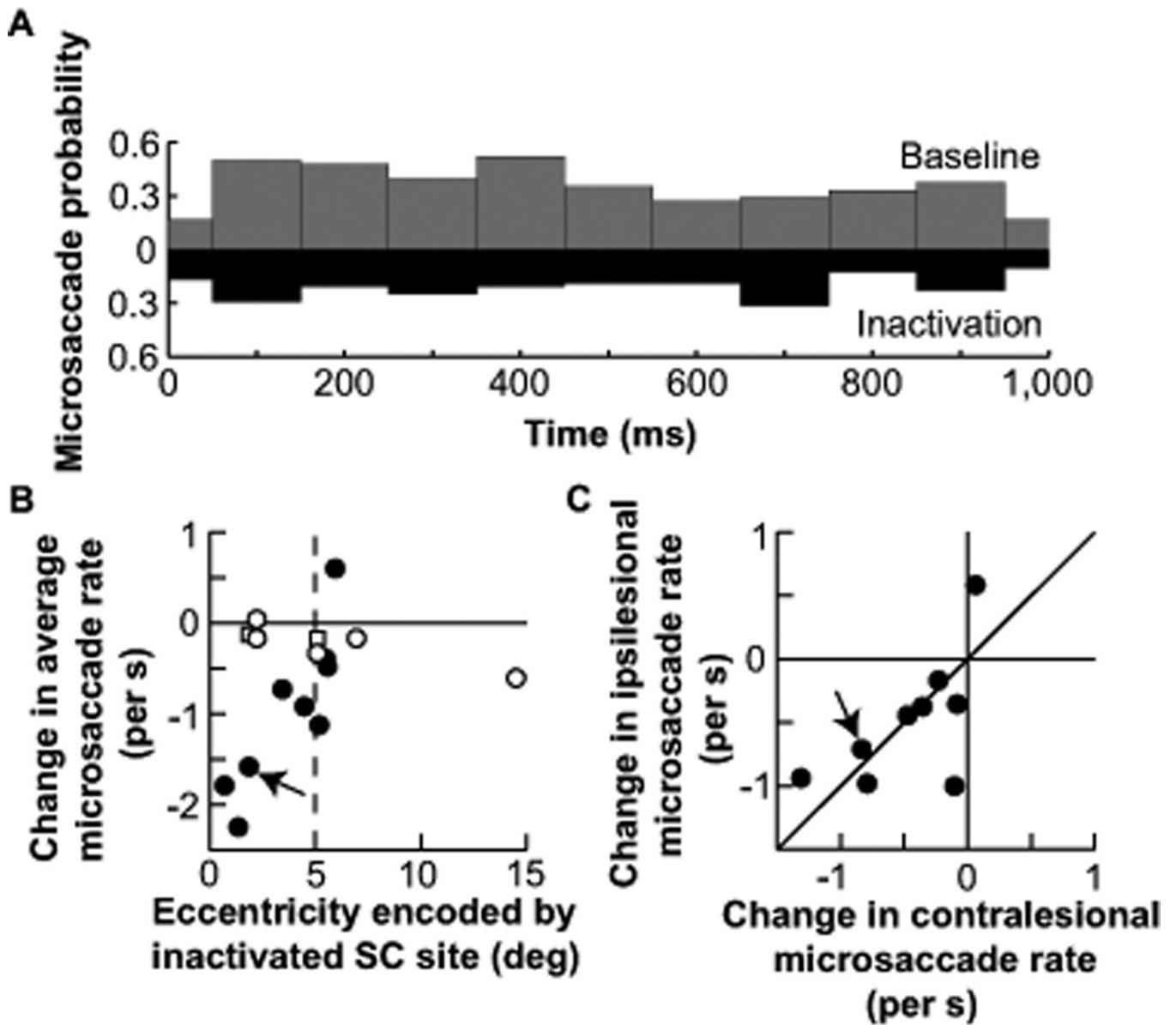


Fig. 3.

A causal role for the SC in microsaccade generation. **A**, Microsaccade probability during one second of fixation before (gray) and after (black) SC inactivation in one experiment (from monkey A; 18). Inactivation reduced microsaccade rate. **B**, Change in average microsaccade rate as a result of SC inactivation (average inactivation rate minus average baseline rate). Inactivation of the most central (i.e. rostral) SC sites caused the biggest reductions in microsaccades. Filled symbols indicate changes with $p < 0.05$ (ranksum test, $N = 48$ trials for baseline, $N = 48$ trials for inactivation; average p -value across filled symbols: 0.018). Squares indicate saline controls, which did not influence microsaccade rate. For a plot of absolute microsaccade rates before and after inactivation (also separated by monkey), see Fig. S7. **C**, Inactivation reduced both contralesional and ipsilesional microsaccades. For the experiments with a significant change in **B** ($N = 9/14$ experiments), data are plotted separately for contralesional and ipsilesional microsaccades. 8/9 experiments fell in the lower left quadrant.

Arrows in **B**, **C** point to the sample experiment of **A**, performed at the same SC site as a subsequent saline control (square at the same eccentricity in **B**).

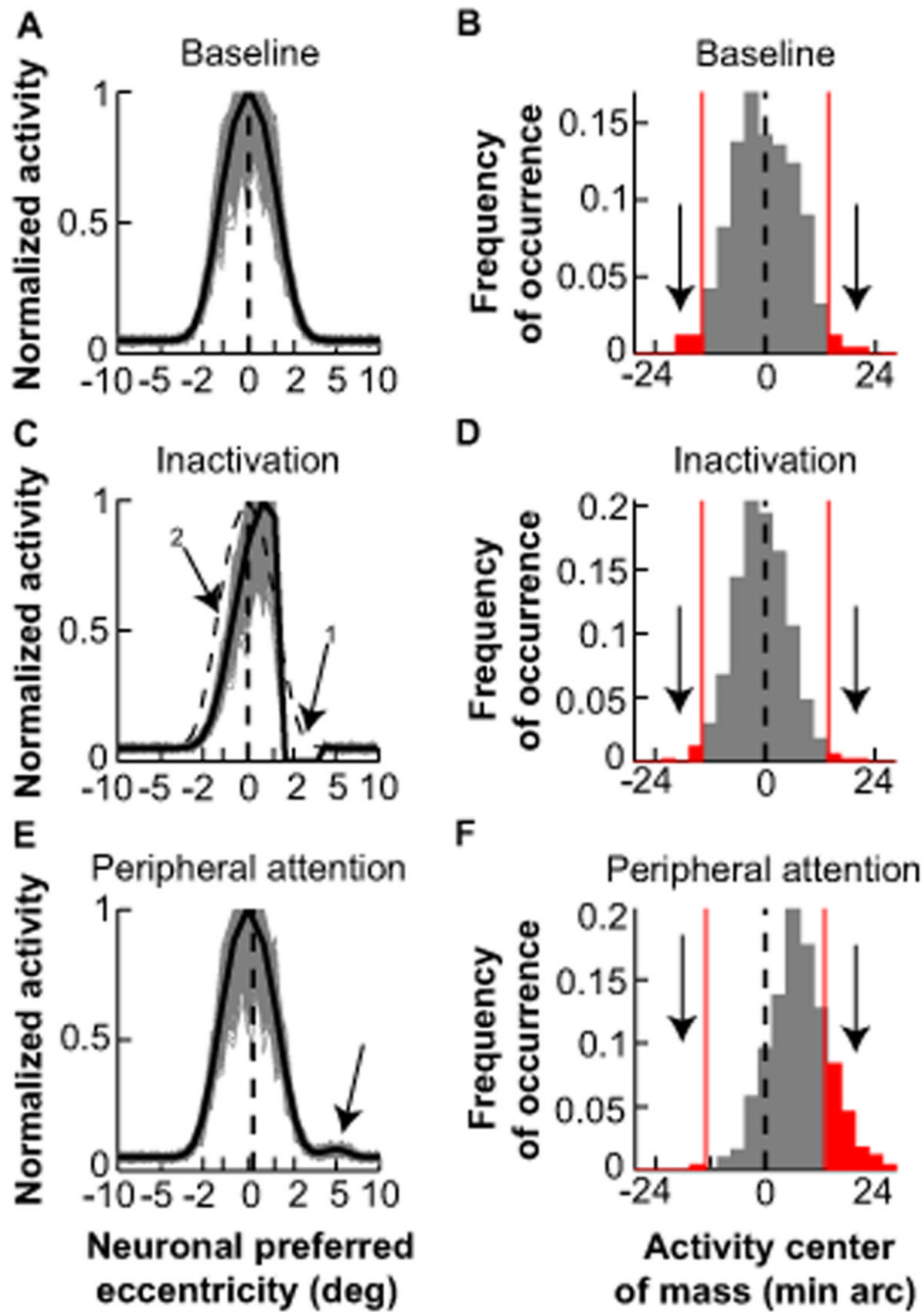


Fig. 4.

A model of goal representation by the SC accounts for microsaccade generation. **A**, Bilateral, one-dimensional SC map with activity representing the fixated goal. Activity is centered on neurons representing the central visual field (dashed black line). Gray traces show activity from 500 iterations of the model with each SC “neuron” exhibiting normally distributed activity (18). Negative values correspond to left, positive to right. **B**, The instantaneous center of mass of SC activity in **A** was variable but had zero mean. Saccades are triggered when this center of mass deviates beyond a certain threshold (for example, red lines indicating 2 s.d.). **C**, Simulating the effect of inactivating neurons representing $\sim 2.5^\circ$ (arrow 1). In the steady-state, inactivation reduced the overall level of SC activity even on the intact side (arrow 2), but

activity remained balanced bilaterally (vertical dashed line) (24). The dashed activity profile shows baseline. **D**, The distribution of SC activity center of mass was narrower than in **B**, but still had zero mean, explaining the reduction in both contralesional and ipsilesional microsaccades. For this simulation, there was a ~50% reduction in the frequency of deviations beyond the threshold of **B** (consistent with our experiments; Fig. S7). **E, F**, Simulating the momentary effects of a covert attention shift to a peripheral site at $\sim 5^\circ$ by introducing an increase in activity at this site (18). The average locus of activity was biased toward the peripheral site (dashed line in **E**), resulting in a higher probability of deviations from fixation towards the peripheral site than away from it (**F**).